

Corrections for the Lutz–Kelker Bias for Galactic Masers

A.S. Stepanishchev¹ and V.V. Bobylev^{1,2}

¹ *Pulkovo Astronomical Observatory, Russian Academy of Sciences*

² *Sobolev Astronomical Institute, St. Petersburg State University, Russia*

Abstract—Based on published data, we have collected information about Galactic maser sources with measured distances. In particular, 44 Galactic maser sources located in star-forming regions have trigonometric parallaxes, proper motions, and radial velocities. In addition, ten more radio sources with incomplete information are known, but their parallaxes have been measured with a high accuracy. For all 54 sources, we have calculated the corrections for the well-known Lutz-Kelker bias. Based on a sample of 44 sources, we have refined the parameters of the Galactic rotation curve. Thus, at $R_0 = 8$ kpc, the peculiar velocity components for the Sun are $(U_\odot, V_\odot, W_\odot) = (7.5, 17.6, 8.4) \pm (1.2, 1.2, 1.2)$ km s⁻¹ and the angular velocity components are $\omega_0 = -28.7 \pm 0.5$ km s⁻¹ kpc⁻¹, $\omega'_0 = +4.17 \pm 0.10$ km s⁻¹ kpc⁻², and $\omega''_0 = -0.87 \pm 0.06$ km s⁻¹ kpc⁻³. The corresponding Oort constants are $A = 16.7 \pm 0.6$ km s⁻¹ kpc⁻¹ and $B = -12.0 \pm 1.0$ km s⁻¹ kpc⁻¹; the circular rotation velocity of the solar neighborhood around the Galactic center is $V_0 = 230 \pm 16$ km s⁻¹. We have found that the corrections for the Lutz-Kelker bias affect the determination of the angular velocity ω_0 most strongly; their effect on the remaining parameters is statistically insignificant. Within the model of a two-armed spiral pattern, we have determined the pattern pitch angle $i = -6.^\circ 5$ and the phase of the Sun in the spiral wave $\chi_0 = 150^\circ$.

1 INTRODUCTION

The observed velocities of various young Galactic objects (HI clouds, OB stars, young open star clusters) are used to study the kinematics of the Galaxy and the spiral structure of the Galactic disk (Bobylev et al. 2008).

For this task, Galactic maser sources with trigonometric parallaxes measured by VLBI are extremely important (Reid et al. 2009a; McMillan and Binney 2010; Bobylev and Bajkova 2010; Stepanishchev and Bobylev 2010). We have in mind the maser sources associated with the youngest Galactic stellar objects (either protostellar objects of various masses, or very massive supergiants, or T Tauri stars). The number of measured parallaxes for such masers already exceeds 50 and with a complete data set (with proper motions and radial velocities) is 44.

Studying their distribution and kinematics with allowance made for the distance errors is of great importance. First of all, it is necessary to take into account the Lutz–Kelker (1973) bias. The corrections for this bias usually play an important role in determining the trigonometric parallaxes by optical methods, when the reference objects are distant stars rather than extragalactic sources. In this case, a procedure for absolutizing the

measured relative parallaxes is needed. For this purpose, the corrections calculated from the Lutz–Kelker bias are usually applied.

In the case of Galactic maser sources, the situation is different. Their trigonometric parallaxes are determined by VLBI with referencing directly to distant quasars (two or three quasars are commonly used). Therefore, such parallaxes are immediately obtained as absolute ones.

At the same time, the VLBI parallaxes of masers were measured with a certain random error that is, on average, very small, about 5%. However, there are exceptions and, in several cases, the error exceeds 20%. As is well known (Lutz and Kelker 1973), the knowledge of the true parallax depends strongly on the relative error of the measured parallax. It can be surmised that the parameters of the Galactic rotation curve and the parameters of the spiral density wave determined from maser sources can be distorted because of the uncertainties in their distances.

Great experience in taking into account the Lutz-Kelker bias has been gained. We will point out only some of the papers. Hanson (1979) applied the method in practice to calibrate the luminosity based on trigonometric parallaxes. In the literature, the method is occasionally called the Lutz-Kelker-Hanson method. Maíz-Apellániz (2001) determined such corrections for O-B5 stars with trigonometric parallaxes from Hipparcos (1997), with the Sun’s height above the Galactic plane having been taken into account. Verbiest et al. (2010) proposed a modification of the method that took into account the luminosity function as applied to 57 Galactic pulsars with measured trigonometric parallaxes. Note that the Lutz–Kelker bias is a statistical effect. A very accurate model of the expected distribution of stars in the Galaxy is required to properly take the Lutz-Kelker bias into account.

The goal of this paper is to calculate the corrections for the Lutz–Kelker bias for masers with measured trigonometric parallaxes and to study the effect of these corrections on the parameters of the Galactic rotation curve and the parameters of the spiral density wave being determined.

2 METHOD

2.1 Uniform Distribution in Space

In its classical form, the Lutz–Kelker bias refers to a uniform distribution of stars in an infinite space (Lutz and Kelker 1973). We assume that the errors in the distribution of the measured parallax relative to its true value are distributed normally:

$$p(\varpi_0|\varpi) = \frac{1}{\sqrt{2\pi}\sigma} \exp\left(-\frac{(\varpi_0 - \varpi)^2}{2\sigma^2}\right). \quad (1)$$

Here, $\pi = 3.14\dots$, σ is the measurement error of the parallax, ϖ_0 and ϖ are the measured and true parallaxes, respectively. We are interested in the distribution of true parallaxes ϖ if a sufficient number of stars with a certain measured value of ϖ_0 are available. If the stars are uniformly distributed in space, then their number in an interval $(r, r + dr)$ is

$$N(r)dr = 4\pi r^2 dr, \quad (2)$$

or

$$N(\varpi)d\varpi = \frac{4\pi d\varpi}{\varpi^4}. \quad (3)$$

According to the Bayes theorem,

$$p(\varpi|\varpi_0) = \frac{p(\varpi_0|\varpi)p(\varpi)}{p(\varpi_0)}, \quad (4)$$

where $p(\varpi_0)$ may be set equal to a constant. We find that

$$p(\varpi|\varpi_0) = \frac{\kappa}{\varpi^4} \exp\left(-\frac{(\varpi_0 - \varpi)^2}{2\sigma^2}\right). \quad (5)$$

The constant κ is chosen in such a way that the normalization condition is fulfilled:

$$\int_{\varpi_{min}}^{\infty} p(\varpi|\varpi_0)d\varpi = 1. \quad (6)$$

The lower limit ϖ_{min} implies the maximum distance at which a given star can be observed in principle from the considerations of the stellar system's size and the telescope's limiting magnitude. In the case of integration from zero, the integral diverges. This reflects an infinite number of stars in an infinite space for the chosen uniform distribution.

The parallax corrected for the Lutz–Kelker bias is the expectation of distribution (5):

$$\varpi_{corr} = \int_{\varpi_{min}}^{\infty} \varpi p(\varpi|\varpi_0)d\varpi. \quad (7)$$

2.2 An Exponential Disk with an Observer at the Periphery

Our objective is to study the objects distributed in the Galactic disk. We assume an exponential density distribution along the Galactic radius, with the distribution along the vertical Z axis following the law of the hyperbolic secant squared:

$$\rho(R) = \rho_0 \exp\left(-\frac{R}{h}\right) \text{ch}^{-2}\left(\frac{Z}{Z_0}\right), \quad h = 3 \text{ kpc}, \quad Z_0 = 0.25 \text{ kpc}, \quad (8)$$

where R is the Galactocentric distance, h and Z_0 are the radial and vertical scale lengths of the disk, respectively; the constant ρ_0 , the density at the center, is a scale factor and its value is of no importance for our problem. The Sun is at $R_0 = 8$ kpc from the Galactic center. When observing from the Sun along the Galactic longitude l , the density distribution takes the form

$$\rho(r, l) = \rho_0 \exp\left(-\frac{\sqrt{(r \cos l - R_0)^2 + r^2 \sin^2 l}}{h}\right). \quad (9)$$

The parallax corrected for the Lutz–Kelker bias is calculated from (7) with the distribution of true parallaxes at given observables:

$$p(\varpi|\varpi_0) \propto \frac{\rho(r, l)}{\varpi^4} \exp\left(-\frac{1}{2} \frac{(\varpi - \varpi_0)^2}{\sigma^2}\right). \quad (10)$$

Таблица 1: Data on the sources that were not included in the “kinematic” sample

Source	α	δ	$\varpi(\sigma_\varpi)$	$\mu_\alpha^*(\sigma_{\mu_\alpha})$	$\mu_\delta(\sigma_{\mu_\delta})$	$V_r(\sigma_{V_r})$	Ref
G 23.66–0.13	278.7149	–8.3059	.313(.039)	–1.32(.02)	–2.96(.03)	83(3)	(a)
G 9.62+0.20	271.5611	–20.5255	.194(.023)	–.58(.05)	–2.49(.27)	0.1(2)	(b)
Sgr B2N	266.8330	–28.3720	.128(.015)	–.32(.05)	–4.69(.11)	64(5)	(c)
Sgr B2M	266.8340	–28.3845	.130(.012)	–1.23(.04)	–3.84(.11)	61(5)	(c)
IRAS 20126+41	303.6084	41.2257	.61(.02)	–2.0(.1)	1.0(.1)	–3.5(4)	(d)
G 48.61+0.02	290.1299	13.9237	.199(.007)	–2.76(.04)	–5.28(.11)	19(1)	(e)
MSXDC G034.4+0	283.3292	1.4022	.643(.049)	–.25(.18)	.00(.18)	57(5)	(f)
EC 95	277.4912	1.2128	2.41(.02)	.70(.02)	–3.64(.10)	–	(g)
IRAS 05137+3919	79.3073	39.3722	.086(.027)	.30(.10)	–.89(.27)	–26(3)	(h)
G 27.36–0.16	280.4627	–5.0287	.125(.042)	–1.81(.08)	–4.11(.26)	92.2(5)	(i)

Note. α and δ are given in degrees, the parallax ϖ is in mas, $\mu_\alpha^* = \mu_\alpha \cos \delta$ and μ_δ are in mas yr^{–1}, the radial velocity $V_r = V_r(LSR)$ is in km s^{–1}; the letters mark the references to papers: (a) Bartkiewicz et al. (2008); (b) Sanna et al. (2009); (c) Reid et al. (2009); (d) Moscadelli et al. (2011); (e) Nagayama et al. (2011b); (f) Kurayama et al. (2011); (g) Dzib et al. (2010); (h) Honma et al. (2011); (i) Xu et al. (2011).

3 DATA

The trigonometric parallaxes and proper motions of Galactic maser sources are determined by several research groups using long-term VLBI observations. These include the Japanese VERA (VLBI Exploration of Radio Astrometry) project on the observation of Galactic H₂O maser sources at 22 GHz and SiO masers (these are very few among the young objects) at 43 GHz. Note that the higher the frequency, the higher the resolution and the more accurate the observations. Methanol (CH₃OH) masers are observed at 12 GHz using the American NRAO VLBA and at 6.7 GHz using the European VLBI Network. At present, Galactic masers are observed by these groups of researchers within the unified BeSSeL project (Brunthaler et al. 2011) aimed at studying the Galactic structure. VLBI observations of a number of young radio stars in continuum at 8.4 GHz (Dzib et al. 2010) are also conducted to study the structure and kinematics of the solar neighborhood (the Gould Belt, molecular clouds).

Bobylev and Bajkova (2010) and Stepanishchev and Bobylev (2011) analyzed a sample of 28 masers with measured trigonometric parallaxes drawn from published data. By now, the amount of such data has increased considerably—about 20 new measurements in various star-forming regions have been published. First of all, we use the input data on 44 masers with measured trigonometric parallaxes, proper motions, and radial velocities from Bajkova and Bobylev (2012), where corresponding references and explanations are given. We arbitrarily call this sample “kinematic”, because on its basis we determine the Galactic rotation parameters.

Table 1 gives the parameters of the sources most of which have small relative errors in the parallaxes, but, for various reasons, they were not included in the “kinematic” sample. Two sources are almost at the Galactic center, Sgr B2N and Sgr B2M (Read

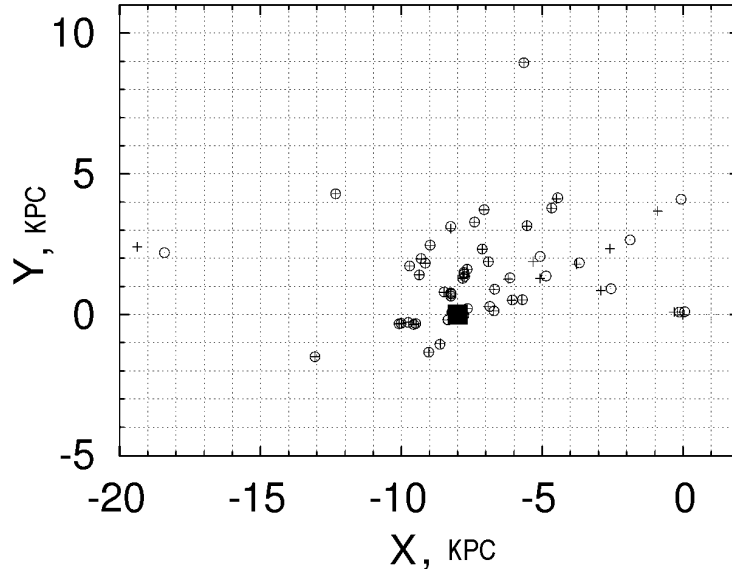


Рис. 1: Projections of masers onto the Galactic plane (XY) from the observed data (crosses) and corrected for the Lutz-Kelker bias (circles); the large filled square marks the position of the Sun; the Galactic Center is at the coordinate origin.

et al. 2009a). Other sources have large ($>40 \text{ km s}^{-1}$) residual velocities: these include G23.66.0.13 (Bartkiewicz et al. 2008), MSXDC G034.43+00.24 (Kurayama et al. 2011), G48.61+0.02 (Nagayama et al. 2011), and IRAS 20126+4104 (Moscadelli et al. 2011). Since the star-forming region G9.62+0.20 (Sanna et al. 2009) is closely connected with the 3-kpc spiral arm, it has a large peculiar Galactocentric radial velocity, $|V_R| \approx 50 \text{ km s}^{-1}$. In addition, we included the radio star EC 95 (Dzib et al. 2010) in our sample, for which there are no radial velocity measurements as yet. Its VLBI observations were carried out in continuum at 8.42 GHz. It is hypothesized that this is a binary system consisting of a Herbig-Haro protostar with a mass of about $4 - 5 M_{\odot}$ and a T Tauri low-mass companion.

The stars from Table 1, especially those farthest from the Sun, are of interest in studying the effect of the Lutz-Kelker bias on the determination of the spiral-structure parameters.

4 RESULTS AND DISCUSSION

The observed (ϖ_{obs}) and Lutz-Kelker-biascorrected (ϖ_{corr}) parallaxes for all 54 maser sources are given in Table 2; their distribution in projection onto the Galactic XY plane is shown in Figs. 1 and 2. As can be seen from Table 2, for most of the maser sources, the calculated Lutz-Kelker bias corrections are negative (the heliocentric distances to them should be increased). The correction is largest for IRAS 16293–2422, but this source is one of the closest to the Sun. Therefore, the correction found has no critical effect on the determination of the (distance-dependent) parameters under consideration. As can

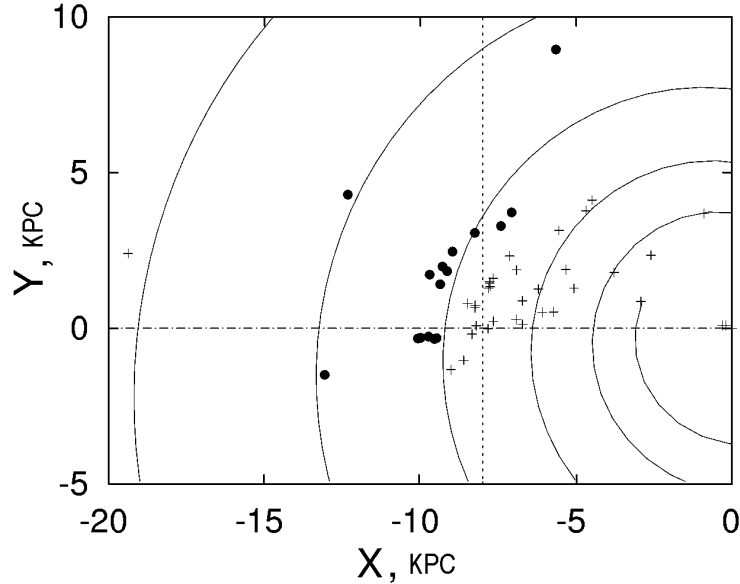


Рис. 2: Two-armed spiral pattern constructed from masers in the Perseus and Outer Arms (thick circles); the remaining objects from our list are indicated by the crosses.

be seen from Fig. 1, a significant change in the distance is achieved for several sources near the Galactic center. The source farthest from the Sun, IRAS 05137+39, is greatest interest. The relative error in the parallax for it is $\approx 30\%$; since the source is close to the direction of the Galactic anticenter, the correction for the Lutz-Kelker bias is positive (its heliocentric distance should be reduced).

Figure 1 clearly illustrates the essence of the method. More specifically, the existence of small measurement errors in the parallaxes gives grounds to expect that the most probable distance to a star should be closer to the region with the highest density of stars (in our case, this is the Galactic center region).

4.1 Spiral Pattern

The parameters of the spiral pattern were determined by the method described in Stepanishchev and Bobylev (2011). The essence of the method consists in the following. We proceed from the well-known equation (Lin and Shu 1964)

$$\chi = m(\text{ctg } i \cdot \ln\{R/R_0\} - \theta) + \chi_0, \quad (11)$$

where χ is the phase of the object in the spiral density wave, χ_0 is the phase of the Sun in the spiral wave, R is the distance from the object to the Galactic rotation axis, θ is the Galactocentric longitude of the object, and m is the number of spiral arms (here, we take $m = 2$). Having chosen two or three groups of objects located along the arms, we estimate the most probable phase of the Sun and the pitch angle of the spiral pattern defined by Eq. (11). For this purpose, we search for the minimum of the functional

$$\zeta^2(i, \chi_0) = \sum (p_j \chi_j)^2, \quad (12)$$

where χ_j is the phase of the j th object reduced to the range $(-\pi/2, \pi/2)$ and p_j is the weight that is chosen based on the number of objects in a given arm in such a way that all arms have the same weight. Here, the masers are assumed to be theoretically concentrated to the spiral arm centers, i.e., the sum of the squares of the objects' phases in the density wave is minimized by taking into account the fact that the phase $\chi = 0^\circ$ corresponds to the arm center.

Owing to the increase in the amount of observational data, these parameters can be calculated with a higher accuracy. Thus, three masers are already known in the Outer Arm against two in the previous paper, while eleven masers are known in the Perseus Arm against seven. In Fig. 2, the objects involved in choosing the model parameters are indicated by the filled circles and the remaining ones are indicated by the crosses. The pitch angle and the Sun's phase were found to be, respectively, $i = -6^\circ.5$ and $\chi_0 = 150^\circ$.

Since the Lutz-Kelker bias corrections for most of the masers belonging to the spiral arms (from which the parameters of the spiral pattern were determined) are insignificant, they were disregarded in the case under consideration. Note once again the source IRAS 05137+39, which is behind the Outer Arm (at ≈ 20 kpc from the Galactic center). It was not used in choosing the model parameters; nevertheless, it falls nicely on the logarithmic spiral fitted into the Perseus and Outer Arms (Fig. 1 and Fig. 2). In their kinematic analysis of a sample of Galactic masers, Bajkova and Bobylev (2012) found a slightly smaller pitch angle of the spiral wave, $i = -5_{-0.9}^{+0.2^\circ}$ (for $m = 2$), and a phase of the Sun in the spiral wave fairly close to our result, $\chi_\odot = -147_{-17}^{+3^\circ}$ (measured from the Carina-Sagittarius Arm). At the same time, the spiral pitch angle we derived differs significantly from the result of analyzing the samples of masers in the Perseus and Outer Arms obtained by Sakai et al. (2012) based on a different method (with a separate analysis of each arm). These authors found $i = -17^\circ.8 \pm 1^\circ.7$ for the Perseus Arm and $i = -11^\circ.6$ for the Outer Arm. This discrepancy in determining the pitch angle can be explained by the fact that the results of Sakai et al. (2012) more closely correspond to the four-armed model of the spiral pattern (in our case, we will then have $i = -13^\circ$). On the whole, we can conclude that considerably larger statistics is required for a reliable determination of the spiral pattern parameters.

4.2 Galactic Rotation Parameters

First, we redetermined the parameters of the Galactic rotation curve using data on 44 masers. Our technique of its determination based on a Taylor expansion of the angular velocity in terms of the Galactocentric distance was described in detail in Bobylev and Bajkova (2010) and Bobylev and Stepanishchev (2011). At a fixed Galactocentric distance of the Sun, $R_0 = 8$ kpc (with an uncertainty of 0.5 kpc), the peculiar velocity components of the Sun $(U_\odot, V_\odot, W_\odot) = (7.5, 17.6, 8.4) \pm (1.2, 1.2, 1.2)$ km s $^{-1}$ and the following parameters of the Galactic rotation curve were obtained:

$$\begin{aligned}\omega_0 &= -28.7 \pm 0.5 \text{ km s}^{-1} \text{ kpc}^{-1}, \\ \omega'_0 &= +4.17 \pm 0.10 \text{ km s}^{-1} \text{ kpc}^{-2}, \\ \omega''_0 &= -0.87 \pm 0.06 \text{ km s}^{-1} \text{ kpc}^{-3},\end{aligned}\tag{13}$$

where ω_0 is the angular velocity of Galactic rotation at $R = R_0$, ω'_0 and ω''_0 are its corresponding derivatives. The Oort constants are $A = 16.7 \pm 0.6 \text{ km s}^{-1} \text{ kpc}^{-1}$ and $B = -12.0 \pm 1.0 \text{ km s}^{-1} \text{ kpc}^{-1}$; the circular rotation velocity of the solar neighborhood around the Galactic center is $V_0 = 230 \pm 16 \text{ km s}^{-1}$.

Note that Stepanishchev and Bobylev (2011) found the analogous parameters using only 28 masers to be the following: $(U_\odot, V_\odot, W_\odot) = (8.5, 17.1, 8.9) \pm (1.6, 1.6, 1.6) \text{ km s}^{-1}$, and $\omega_0 = -30.4 \pm 0.7 \text{ km s}^{-1} \text{ kpc}^{-1}$, $\omega'_0 = 4.23 \pm 0.13 \text{ km s}^{-1} \text{ kpc}^{-2}$, $\omega''_0 = -1.01 \pm 0.06 \text{ km s}^{-1} \text{ kpc}^{-3}$. It can be seen that solution (13) is more reliable, because, as would be expected, the random errors of all the parameters being determined decreased. Solution (13) virtually coincides with results of analyzing this sample of masers from Bajkova and Bobylev (2012), where a detailed comparison of these values with the results of other authors can be found.

After applying the Lutz–Kelker correction, we obtained the following parameters of the rotation curve: $(U_\odot, V_\odot, W_\odot) = (6.6, 17.9, 8.5) \pm (1.4, 1.4, 1.4) \text{ km s}^{-1}$ and

$$\begin{aligned}\omega_0 &= -27.5 \pm 0.5 \text{ km s}^{-1} \text{ kpc}^{-1}, \\ \omega'_0 &= +3.98 \pm 0.11 \text{ km s}^{-1} \text{ kpc}^{-2}, \\ \omega''_0 &= -0.83 \pm 0.06 \text{ km s}^{-1} \text{ kpc}^{-3},\end{aligned}\tag{14}$$

Hence we see that after applying the correction, the angular velocity ω_0 changed by about 2.5σ , while its derivatives and the Sun’s peculiar velocity components change within the error limits (i.e., insignificantly).

5 CONCLUSIONS

Based on published data, we collected information about Galactic maser sources with well measured distances. In particular, 44 Galactic maser sources located in star-forming regions have a complete set of kinematic observational data—the VLBI trigonometric parallaxes and proper motions; the mean radial velocities derived from CO observations are also known for them. In addition, ten more radio sources with incomplete information are known, but their parallaxes were measured with a sufficiently high accuracy.

We calculated the corrections for the well-known Lutz–Kelker bias for all 54 sources. For this purpose, we used a model with an exponential star density distribution in the Galactic disk. For several sources farthest from the Sun, these corrections were shown to be appreciable. Using the calculated corrections can be useful, for example, in studying the membership of masers in the Galactic bar or specific spiral arms, etc.

Based on a sample of 44 sources, we refined the parameters of the Galactic rotation curve. At $R_0 = 8 \text{ kpc}$, we determined the peculiar velocity components of the Sun $(U_\odot, V_\odot, W_\odot) = (7.5, 17.6, 8.4) \pm (1.2, 1.2, 1.2) \text{ km s}^{-1}$ and the following parameters: $\omega_0 = -28.7 \pm 0.5 \text{ km s}^{-1} \text{ kpc}^{-1}$, $\omega'_0 = +4.17 \pm 0.10 \text{ km s}^{-1} \text{ kpc}^{-2}$ и $\omega''_0 = -0.87 \pm 0.06 \text{ km s}^{-1} \text{ kpc}^{-3}$. The corresponding Oort constants are $A = 16.7 \pm 0.6 \text{ km s}^{-1} \text{ kpc}^{-1}$ and $B = -12.0 \pm 1.0 \text{ km s}^{-1} \text{ kpc}^{-1}$; the circular rotation velocity of the solar neighborhood around the Galactic center is $V_0 = 230 \pm 16 \text{ km s}^{-1}$. We found that when using our sample, the corrections for the Lutz–Kelker bias affect the determination of the angular velocity of Galactic rotation ω_0 (at the 2.5σ level), while these corrections have no statistically

significant effect on the other model parameters being determined. This is primarily due to the high accuracy of the measured trigonometric parallaxes for the masers used. Within the model of a two-armed spiral pattern, we determined the pattern pitch angle $i = -6^\circ.5$ and the phase of the Sun in the spiral wave $\chi_0 = 150^\circ$.

ACKNOWLEDGMENTS

This work was supported in part by the “Origin, Structure, and Evolution of Objects of the Universe” Program of the Presidium of the Russian Academy of Sciences and the Program for State Support of Leading Scientific Schools of the Russian Federation (project no. NSh-3645.2010.2 “Multiwavelength Astrophysical Research”).

REFERENCES

1. A.T. Bajkova and V.V. Bobylev, *Astron. Lett.* **38**, (2012).
2. A. Bartkiewicz, A. Brunthaler, M. Szymczak, *et al.*, *Astron. Astrophys.* **490**, 787 (2008).
3. V.V. Bobylev, A.T. Bajkova, and A.S. Stepanishchev, *Astron. Lett.* **34**, 515 (2008).
4. V.V. Bobylev and A.T. Bajkova, *Mon. Not. R. Astron. Soc.* **408**, 1788 (2010).
5. A. Brunthaler, M. Reid, K. M. Menten, *et al.*, *Astron. Nachr.* **332**, 461 (2011).
6. S. Dzib, L. Loinard, A. J. Mioduszewski, *et al.*, *Astrophys. J.* **718**, 610 (2010).
7. R.B. Hanson, *Mon. Not. R. Astron. Soc.* **186**, 875 (1979).
8. HIPPARCOS and Tycho Catalogues, ESA SP-1200 (1997).
9. T. Honma, T. Hirota, Y. Kan-ya, *et al.*, *Publ. Astron. Soc. Jpn.* **63**, 17 (2011).
10. T. Kurayama, A. Nakagawa, S. Sawada-Satoh, *et al.*, *Publ. Astron. Soc. Jpn.* **63**, 513 (2011).
11. C.C. Lin and F.H. Shu, *Astroph. J.* **140**, 646 (1964).
12. T.E. Lutz and D.H. Kelker, *Publ. Astron. Soc. Pacif.* **85**, 573 (1973).
13. J. Maíz-Apellániz, *Astron. J.* **121**, 2737 (2001).
14. P.J. McMillan and J.J. Binney, *Mon. Not. R. Astron. Soc.* **402**, 934 (2010).
15. L. Moscadelli, R. Cesaroni, M. J. Rioja, *et al.*, *Astron. Astrophys.* **526**, 66 (2011).
16. T. Nagayama, T. Omodaka, T. Handa, *et al.*, *Publ. Astron. Soc. Jpn.* **63**, 719 (2011b).
17. M.J. Reid, K.M. Menten, X.W. Zheng, *et al.*, *Astrophys. J.* **700**, 137 (2009a).
18. M. Reid, K.M. Menten, X.W. Zheng, *et al.*, *Astrophys. J.* **705**, 1548 (2009b).
19. N. Sakai, M. Honma, H. Nakanishi, *et al.*, *Publ. Astron. Soc. Jpn.* **64**, 108 (2012).
20. A. Sanna, M.J. Reid, L. Moscadelli, *et al.*, *Astrophys. J.* **706**, 464 (2009).
21. A.S. Stepanishchev and V.V. Bobylev, *Astron. Lett.* **37**, 254 (2011).
22. J.P.W. Verbiest, D.R. Lorimer, and M.A. McLaughlin, *Mon. Not. R. Astron. Soc.* **405**, 564 (2010).
23. Y. Xu, L. Moscadelli, M.J. Reid, *et al.*, *Astrophys. J.* **733**, 25 (2011).

Таблица 2: Observed and Lutz–Kelker-bias-corrected parallaxes (in mas)

Source	ϖ_{obs}	ϖ_{corr}	Correction
G 121.28+0.65	1.077 (0.039)	1.072	-0.005
IRAS 00420+5530	0.460 (0.010)	0.460	0.000
G 123.05−6.31	0.421 (0.022)	0.419	-0.002
S Per	0.413 (0.017)	0.411	-0.002
G 133.94+1.04	0.512 (0.007)	0.512	0.000
WB89−437	0.164 (0.006)	0.164	0.000
SVS13 f1+f2	4.250 (0.320)	4.158	-0.092
Ori KL H2O	2.425 (0.035)	2.423	-0.002
Ori KL SiO	2.390 (0.030)	2.389	-0.001
G 189.78+0.34	0.476 (0.006)	0.476	0.000
G 188.95+0.89	0.569 (0.034)	0.562	-0.007
G 188.78+1.03	0.496 (0.031)	0.490	-0.006
G 192.60−0.05	0.628 (0.027)	0.624	-0.004
G 196.45−1.68	0.189 (0.008)	0.188	-0.001
VY CMa	0.830 (0.080)	0.803	-0.027
G 232.62+0.99	0.596 (0.035)	0.589	-0.007
G 14.33−0.64	0.893 (0.101)	0.839	-0.054
G 23.43−0.18	0.170 (0.032)	0.143	-0.027
G 23.01−0.41	0.218 (0.017)	0.211	-0.007
G 35.20−0.74	0.456 (0.045)	0.435	-0.021
G 35.20−1.74	0.306 (0.045)	0.274	-0.032
IRAS 19213+1723	0.251 (0.010)	0.249	-0.002
W51 Main/South	0.185 (0.010)	0.183	-0.002
G 59.78+0.06	0.463 (0.020)	0.459	-0.004
G 94.58−1.79	0.326 (0.032)	0.315	-0.011
L 1204 G	1.309 (0.047)	1.303	-0.006
G 108.18+5.51	1.289 (0.153)	1.217	-0.072
G 109.86+2.10	1.430 (0.080)	1.412	-0.018
G 111.53+0.76	0.378 (0.017)	0.375	-0.003
IRAS 16293−2422	5.600 (1.100)	4.425	-1.175
L 1448 C	4.310 (0.330)	4.214	-0.096
G 5.89−0.39	0.780 (0.050)	0.765	-0.015
Onsala1	0.404 (0.017)	0.401	-0.003
Onsala2	0.261 (0.009)	0.260	-0.001
G 12.89+0.49	0.428 (0.022)	0.423	-0.005
G 15.03−0.67	0.505 (0.033)	0.495	-0.010
G 192.16−3.84	0.660 (0.040)	0.652	-0.008
G 75.30+1.32	0.108 (0.005)	0.108	0.000
W75 N	0.772 (0.042)	0.763	-0.009
DR 21	0.666 (0.035)	0.659	-0.007
DR 20	0.687 (0.038)	0.678	-0.009
IRAS 20290+4052	0.737 (0.062)	0.715	-0.022
AFGL 2591	0.300 (0.010)	0.299	-0.001

Table 2 (the end)

Source	ϖ_{obs}	ϖ_{corr}	Correction
HW9 CepA	1.430 (0.070)	1.417	-0.013
Sgr B2N	0.128 (0.015)	0.122	-0.006
Sgr B2M	0.130 (0.012)	0.126	-0.004
IRAS 05137+3919	0.086 (0.027)	0.093	0.007
G 27.36−0.16	0.125 (0.042)	0.103	-0.022
G 48.61+0.02	0.199 (0.007)	0.198	-0.001
IRAS 20126+4104	0.610 (0.020)	0.608	-0.002
G 9.62+0.19	0.194 (0.023)	0.177	-0.017
MSXDC G034.43+00.24	0.643 (0.049)	0.626	-0.017
G 23.66−0.13	0.313 (0.039)	0.286	-0.027
EC 95	2.410 (0.020)	2.409	-0.001